Mapping of Electron-Hole Excitations in the Charge-Density-Wave System 1T-$TiSe_2$ Using Resonant Inelastic X-Ray Scattering

C. Monney,[1,*] K. J. Zhou,[1,2] H. Cercellier,[3] Z. Vydrova,[4] M. G. Garnier,[4] G. Monney,[4] V. N. Strocov,[1] H. Berger,[5] H. Beck,[4] T. Schmitt,[1] and P. Aebi[4]

[1]*Research Department Synchrotron Radiation and Nanotechnology, Paul Scherrer Institut, CH-5232 Villigen PSI, Switzerland*
[2]*Diamond Light Source, Harwell Science and Innovation Campus, Didcot, Oxfordshire OX11 0DE, United Kingdom*
[3]*Institut Néel, CNRS-UJF, BP 166, 38042 Grenoble, France*
[4]*Département de Physique and Fribourg Center for Nanomaterials, Université de Fribourg, CH-1700 Fribourg, Switzerland*
[5]*EPFL, Institut de Physique de la Matière Condensée, CH-1015 Lausanne, Switzerland*

In high-resolution resonant inelastic x-ray scattering at the Ti L edge of the charge-density-wave system 1T-$TiSe_2$, we observe sharp low energy loss peaks from electron-hole pair excitations developing at low temperature. These excitations are strongly dispersing as a function of the transferred momentum of light. We show that the unoccupied bands close to the Fermi level can effectively be probed in this broadband material. Furthermore, we extract the order parameter of the charge-density-wave phase from temperature-dependent measurements.

A detailed knowledge of the band structure of crystalline solids near their Fermi energy is essential for describing and understanding their low energy electronic properties. For this purpose, momentum $\vec{k}$-resolved spectroscopic probes are necessary and angle-resolved photoemission spectroscopy (ARPES), which measures the one-particle spectral function, is particularly appropriate, given its excellent energy resolution. However, ARPES provides information only on the occupied band structure, especially deficient in the case of gapped systems. Inverse photoemission is a possible candidate for directly probing the unoccupied band structure but offers only a poor energy resolution. More insight in the band structure around the Fermi energy can be gained from two-particle spectroscopic techniques, like electron energy loss spectroscopy, which can measure electron-hole excitations across the gap. However, this technique is demanding in sample preparation, due to the limited escape depth of electrons.

Resonant inelastic x-ray scattering (RIXS) is a good answer to this issue, given its rapid technical progress and its great potential [1–6]. As a photon-in and photon-out technique, it does not require a complicated sample preparation, and it is bulk sensitive. Similarly to electron energy loss spectroscopy, it measures electron-hole excitations and has early on been shown to give access to the band structure of insulating and semimetallic materials by varying the incident energy of the photons [7,8]. In these experiments, band mapping was done by assigning peaks in the x-ray absorption spectra (XAS) to high symmetry points in the unoccupied band structure and linking them to particular $\vec{k}$-resolved positions in the occupied band structure, invoking momentum conservation in the scattering process. However, this procedure has been applied on a typical energy scale of 5 to 10 eV with an energy resolution of about 0.5 to 1 eV.

In this Letter, we demonstrate that electron-hole excitations in a charge-density-wave (CDW) material can directly be mapped with RIXS by changing the momentum of light. With this method, sharp electron-hole excitations at low energy loss and with a substantial dispersion are measured in the CDW system 1T-$TiSe_2$. Furthermore, a detailed temperature dependence of these excitations allows us to directly follow the evolution of the CDW gap and its closing over a wide temperature range. This observation of sharp momentum-dispersive peaks in a broadband semimetallic material opens new perspectives for probing the unoccupied states with RIXS.

RIXS experiments were performed at the ADRESS beam line [9] of the Swiss Light Source, Paul Scherrer Institut, using the SAXES spectrometer [10]. RIXS spectra were recorded in typically 4 h acquisition time, achieving a statistics of 150–200 photons in the peak maxima of interest (see below). A scattering angle of 130° was used, and all the spectra were measured with linearly σ-polarized incident light [perpendicular to the scattering plane; see Fig. 1(a)]. The combined energy resolution was 90 meV at the Ti L edge ($\sim$ 460 eV). 1T-$TiSe_2$ single crystals were cleaved [with a surface in the (001) direction] *in situ* at a pressure of about 1×10^{-8} mbar. The crystals were oriented so that the transferred momentum of light lies in the ΓML plane [see Fig. 1(a)] and that the polarization of light lies completely in the Ti plane.

1T-$TiSe_2$ is a quasi-two-dimensional transition metal dichalcogenide, which undergoes at $T_c = 200$ K a second-order phase transition towards a CDW phase [11], the origin of which is still debated [12–15]. Its normal phase band structure is at the edge between a semimetallic and a

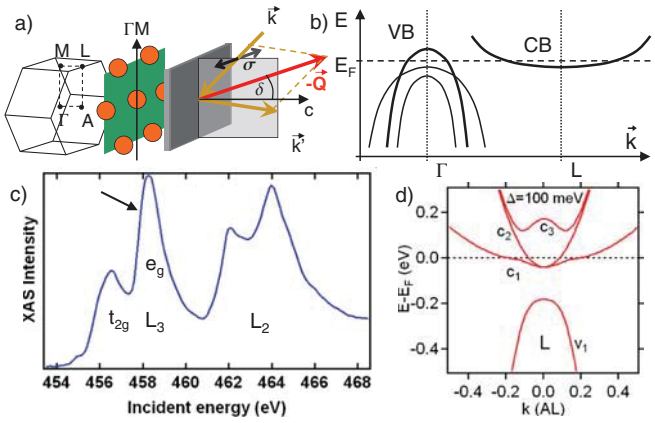

FIG. 1 (color online). (a) Scattering geometry of the experiment with respect to a Ti layer (in the ab plane), with the Brillouin zone of 1T-$TiSe_2$. (b) Schematic band structure near the Fermi level. (c) XAS of 1T-$TiSe_2$ at the L edge for 16 K, in the specular geometry with σ-polarized light (i.e., perpendicular to the scattering plane). (d) Model band structure of 1T-$TiSe_2$ in the CDW phase, where the topmost valence band is coupled with the (three symmetry equivalent) conduction bands [thick lines in (b)] (see the text).

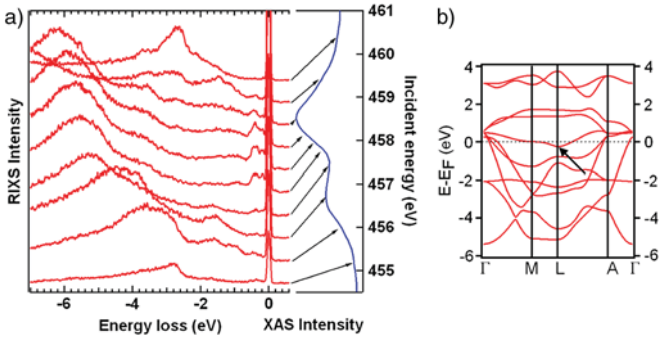

FIG. 2 (color online). (a) Incident energy dependence of the RIXS signal on 1T-$TiSe_2$ (at 16 K, 4° away from specular), measured along the XAS spectrum. (b) Band structure of 1T-$TiSe_2$ calculated with DFT.

semiconducting configuration, actually strongly affected by CDW fluctuations persisting well above T_c [16,17]. Near the Fermi energy, it consists of Se 4p valence bands centered at Γ and of Ti 3d conduction bands at L [see Fig. 1(b) for a schematic picture]. We have recently developed a minimal model, containing the topmost valence band at Γ and three symmetry equivalent conduction bands at L having parabolic dispersions along high symmetry directions [thick lines in Fig. 1(b)], for describing the evolution of this band structure in the CDW phase [18].

An XAS spectrum of 1T-$TiSe_2$ at the L_3 and L_2 edges has been measured at low temperature (16 K) and is shown in Fig. 1(c), being typical for a d^0 system in an octahedral environment (O_h symmetry). At the L_3 edge, the two main peaks are separated by 1.7 eV due to the crystal field splitting and correspond to the t_{2g} (around 456.6 eV) and e_g (around 458.3 eV) manifolds.

Based on this XAS spectrum, we have measured RIXS spectra at different incident energies along the L_3 edge at low temperature (16 K), well in the CDW phase. This corresponds to resonantly exciting electrons from Ti $2p_{3/2}$ core levels with an incident energy $\hbar\omega_i$ to unoccupied d states close to the Fermi energy and to measuring the energy of the photons $\hbar\omega_f$ emitted by the deexcitation of occupied electrons into the core hole. These spectra are shown in Fig. 2(a) in an energy loss scale $\hbar(\omega_f - \omega_i)$. A strong elastic line appears at 0 eV energy loss and the fluorescence structure, already present around −3 eV energy loss (as expected for a semimetal), shifts to higher energies, as the incident energy increases. A few broad peaks can be seen between the fluorescence and the elastic line and are probably due to high energy dd excitations, in which d electrons are excited between different d orbitals. The breadth of these peaks testifies to the dispersive nature of the system. Most interestingly, however, sharper Raman-like peaks (i.e., not moving as the incident energy is changed) are observed close to the elastic line, when the system is excited on the lower energy edge of the e_g peak [see the arrow in Fig. 1(c)]. This behavior is reminiscent of a doped d^0 system, as in $LaAlO_3/SrTiO_3$ heterostructures [19], where the small portion of occupied states can give rise to a weak shoulder precisely at this position (the Ti^{3+} resonance) in the XAS spectrum [19]. Indeed, due to the Ti-Se hybridization and to the presence of a small excess of Ti atoms in its van der Waals gap, 1T-$TiSe_2$ is actually not purely in a d^0 configuration, as one would imagine in a simple ionic picture, but rather in a $d^{0+\alpha}$ configuration, with α being small, of the order of 1% [11]. This is confirmed by the observation of a partially occupied Ti 3d band in 1T-$TiSe_2$ in photoemission at low temperature [16]. As a consequence, we expect that the measured XAS spectrum is the result of the superposition of d^0 and of d^1 configurations, the latter having a much smaller contribution (not visible here) than the former [20]. This observation indicates that these low energy Raman-like peaks are related to the states in the lowest occupied d band. We will now focus on these peculiar low energy peaks to extract information on the electronic structure close to the Fermi energy.

To gain more insight into their origin, we have measured these low energy loss peaks at an incident energy of 457.9 eV (middle of the edge of the e_g peak) and at 16 K as a function of the polar angle δ relative to the specular direction of the sample [see Fig. 1(a)]. This results in changing the direction of the light momentum transferred to the sample, $\vec{Q} = \vec{k}' - \vec{k}$, and thus is modifying the size of its projection on the Ti planes (ab plane), while keeping it in the ΓML plane. The corresponding measured spectra, zooming in on the low energy loss region, are shown in Fig. 3(a). These high statistics measurements reveal different peaks, one of them exhibiting a remarkable dispersion.

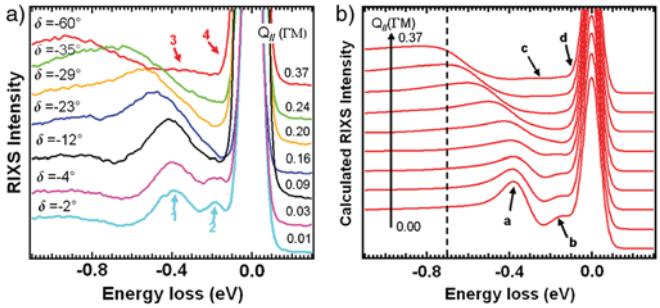

FIG. 3 (color online). (a) Measured RIXS spectra as a function of the polar angle δ, for an incident energy of 457.9 eV and $T = 16$ K. (b) The corresponding calculated RIXS spectra using the band structure in the CDW phase (see the text).

Starting at -0.39 eV close to specular ($\delta = -4°$), an intense sharp peak (1) disperses (and also broadens) strongly to higher energy losses when increasing $|\delta|$. Between this peak and the elastic line appears another sharp and weaker peak (2), at -0.19 eV, which seems not to disperse and quickly disappears in the tail of the former peak, when going away from the specular position. At angular positions close to grazing incidence (high $|\delta|$), where peak (1) reaches -0.9 eV, another broad peak (3) is observed at around -0.36 eV. Finally, in the low energy loss region, a weak additional contribution (4) close to the elastic line may be present at grazing incidence.

In order to understand the nature of these low energy loss peaks in $1T$-$TiSe_2$, we first exclude phonons, as they appear at much smaller energies in this material [22]. Then, $1T$-$TiSe_2$ is a broadband system, without any strong magnetic moments [11]. Therefore, no magnetic excitations are expected at this energy scale. As a consequence, we focus on purely electronic excitations, namely electron-hole excitations near the Fermi level.

Let us first look at the band structure of $1T$-$TiSe_2$ [Fig. 2(b)] in the normal phase (corresponding to the room temperature phase), calculated by density functional theory (DFT) [23]. Although it is known that DFT fails to describe accurately this band structure close to the Fermi level E_F, it provides us with a good starting point for discussion. The bands below E_F have mostly Se $4p$ character [among which are the valence bands described in Fig. 1(b)], while those above E_F have mostly Ti $3d$ character [among which are the conduction bands described in Fig. 1(b)]. At L, the Ti $3d$ conduction band crosses E_F [see the arrow in Fig. 2(b)], providing the d^1 states contributing to the Ti^{3+} XAS. Thus, when doing RIXS at incident energies exciting these states resonantly, one probes the region in k space close to L. However, based on this band structure, no dd excitations are expected around L for energy losses below 1 eV.

Below 200 K, the electronic structure of $1T$-$TiSe_2$ close to E_F is strongly affected by the CDW phase, so that new (backfolded) bands appear, in particular at L. Occupied bands have been evidenced by ARPES and, on this basis, we have developed a model for the electronic structure in the CDW phase, which is characterized by an order parameter Δ (similar to the one of the BCS theory of superconductivity) determining the coupling between the valence and the conduction bands [18]. Figure 1(d) displays such bands in the CDW phase calculated with $\Delta = 100$ meV, obtained by the coupling of the valence band (at Γ) to the three symmetry equivalent conduction bands at L. As shown here, in addition to the original conduction band c_1, the valence band v_1 is now backfolded from Γ to L, as well as conduction bands (c_2, c_3) coming from other L points. Due to the strong hybridization between these bands, the backfolded valence band v_1 possesses a non-negligible d character (in the same way, the conduction bands also possess some p character). This opens new possibilities for interband electron-hole excitations in the RIXS process, respecting the $\Delta L = 0$ selection rule for dipolar transitions.

For simulating RIXS on $1T$-$TiSe_2$, we adopt a simple approach, consisting of calculating the transferred light momentum $\vec{Q}$—and the energy loss $\hbar\omega_{\text{loss}}$—resolved convolution of the dispersions involved in the electron-hole excitations, e.g., $\varepsilon_{v_1}(\vec{k})$ and $\varepsilon_{c_i}(\vec{k}')$, so that the formula reads

$$I_{\text{RIXS}}(\omega_{\text{loss}}, \vec{Q}) \propto \int d\vec{k} \int d\vec{k}' \, \delta(\hbar\omega_{\text{loss}} - \varepsilon_{v_1}(\vec{k}) - \varepsilon_{c_i}(\vec{k}'))\delta(\vec{k} - \vec{k}' - \vec{Q}) N_F(\varepsilon_{v_1}(\vec{k})) \times [1 - N_F(\varepsilon_{c_i}(\vec{k}'))],$$

where the Fermi distribution N_F accounts for the occupied and unoccupied states. As input to this calculation, we use the (renormalized) dispersions $\varepsilon_{v_1}(\vec{k})$, $\varepsilon_{c_i}(\vec{k})$ ($i = 1, 2, 3$) shown in Fig. 1(d), calculated (using the CUBA library [24]) from Ref. [18] using $\Delta = 100$ meV and the band parameters given in Ref. [25]. We consider all the possible inter- and intraband excitations involving these bands. The δ functions above are broadened by a Gaussian profile, representing the instrumental energy resolution [26].

The resulting curves, summing up all electron-hole excitations, are shown in Fig. 3(b). They compare well with the experiment [Fig. 3(a)], the main peaks being reproduced in energy loss position and dispersion. In particular, although many different inter- and intraband excitations contribute, peak (1) in the experiment can be associated to peak (a) in the simulation, which is mainly traced back to the interband excitation between the (backfolded) valence band v_1 and the (backfolded) conduction band c_3 [see Fig. 1(d)]. This peak thereby confirms the existence of the backfolded conduction band c_3, never observed before (only the occupied bands v_1 and c_1 have been observed in ARPES [12]). Furthermore, peak (2) in the experiment, associated to peak (b) in the simulation, is mainly coming from the interband excitation between the conduction bands c_1 and c_2 (which are degenerate at L)

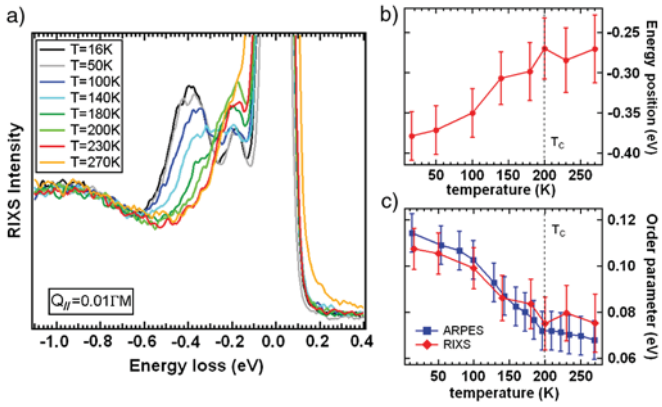

FIG. 4 (color online). RIXS spectra measured (a) at $Q_{\parallel} = 0.01\Gamma M$ as a function of temperature. (b) The energy position of peak (1) measured at $Q_{\parallel} = 0.01\Gamma M$ as a function of temperature and (c) the corresponding order parameter Δ, together with the order parameter derived from ARPES data in Ref. [16] (see the text).

and the (backfolded) conduction band c_3 [see Fig. 1(d)]. At energies far from E_F, the conduction and valence band dispersions are expected to deviate from the ideal parabolic ones. Therefore, the calculated energy loss region higher than 0.7 eV in Fig. 3(b) (left from the dashed line) may exhibit discrepancies in comparison to the experiment in Fig. 3(a).

Having now identified the origin of the dispersive peaks measured in RIXS at low temperature, we can investigate the temperature dependence of the RIXS spectra for our CDW system. Figure 4(a) shows such a temperature dependence for RIXS spectra measured at $Q_{\parallel} = 0.01\Gamma M$. Strong effects both in intensity and peak positions are observed. Peak (1) is strongly suppressed when the temperature increases towards room temperature and, at the same time, it shifts towards the elastic line. The behavior of peak (2) is more difficult to visualize, since it is strongly influenced by peak (1) shifting to smaller energy loss and by the elastic line. Close to the specular direction, the spectrum is dominated by the band behavior close to their extrema (at L). We have fitted the position of peak (1) as a function of temperature [27] and the resulting curve is shown in Fig. 4(b). Its collapse and shifting are direct consequences of the temperature driving the system out of the CDW phase to the normal phase at room temperature. Indeed, the distance between the maxima of the bands v_1 (E_{v_1}) and c_3 (E_{c_3}) is the CDW gap in $1T$-$TiSe_2$ (the original conduction band, c_1, stays at its initial position, acting as a spectator band [18]). It is related to the order parameter of the CDW phase Δ by the relation $E_{c_3} - E_{v_1} = \sqrt{E_G^2 + 12\Delta^2}$ [16]. Using the valence-to-conduction band overlap value (in the normal phase) of $|E_G| = 0.07$ eV [12], the curve for the corresponding order parameter Δ is calculated and shown in Fig. 4(c). It is in good agreement with a similar analysis done in a previous ARPES study [16], for which the main result has been carried over in Fig. 4(c). This confirms further our assignment of peak (1) to the electron-hole excitations across the CDW gap. Actually, the CDW gap is directly measured in this RIXS experiment, since electron-hole excitations between the occupied and unoccupied bands are probed, whereas in the ARPES experiment, the CDW gap was inferred indirectly via the energy position of the conduction band c_1 relative to the one of the backfolded band v_1.

Looking at the RIXS spectra of Fig. 4(a), it is difficult to infer a transition temperature, due to the merging of the two peaks close to the elastic line at higher temperatures. The presence of strong fluctuations of the CDW phase above T_{CDW}, evidenced in photoemission [16], is probably a reason why it is smeared out and why low energy peaks are still present (although weak) in the spectra close to room temperature. This is further supported by the nonzero order parameter above T_c extracted from our data [Fig. 4(c)], which artificially simulates this fluctuation regime, for which a solid theoretical understanding has been given recently [17].

It is interesting to discuss the comparison of the RIXS spectra measured close to specular [Fig. 4(a)] with optical conductivity data of Li *et al.* [28], since in these data, electron-hole excitations are also probed, but for $\vec{Q} = 0\,\text{Å}^{-1}$. Indeed, at 10 K, Li *et al.* observe only one peak at 0.4 eV, which decreases in intensity for higher temperatures, and these authors interpret it as a consequence of the CDW gap opening. This is in agreement with our interpretation of peak (1). Looking closer at their spectra, one may distinguish another weak feature at lower energy, which could have the same origin as our peak (2). Obviously, the matrix elements of RIXS are in this particular case more favorable, since peak (2) is clearly visible in our spectra.

It is at first sight very remarkable to observe such strong band dispersion effects with so sharp peaks in RIXS data obtained at the L edge. On the one hand, in strongly correlated systems, which are particularly investigated with RIXS nowadays for their magnetic properties, the weakly screened core hole at the L edge gives rise to strong excitonic effects and opens channels for relaxation of the excited electron in the intermediate state. These effects make the electron-hole excitation mapping more difficult or even impossible [29]. On the other hand, one is usually expecting in the case of dispersive systems to observe broad features in the RIXS spectra, which makes it difficult to get information on the band structure. Furthermore, for metallic (or semimetallic) materials, the fluorescence may dominate the spectra and hide any low energy excitation. However, as emphasized by early RIXS works [8], in the case of weakly correlated materials, the momentum $\vec{k}$ is mostly conserved in the RIXS process, which has to be seen as a one-step process with virtual intermediate states. This allows then for interpretation of the RIXS spectra in terms of electron-hole excitation mapping, as ideally

illustrated with the case of $1T$-$TiSe_2$, making it possible to retrieve information on unoccupied states.

In conclusion, we have performed resonant inelastic x-ray scattering measurements at the L edge of Ti on the charge-density-wave material $1T$-$TiSe_2$. Peculiar low energy excitations are evidenced when the system is excited at the main Ti^{3+} resonance. These low energy excitations disperse as a function of the transferred momentum of light $\vec{Q}$ and are shown to be inter- and intraband electron-hole excitations. This emphasizes the great potential of $\vec{Q}$-dependent RIXS for doing band mapping in broadband materials. Furthermore, temperature-dependent RIXS spectra permit us to directly follow the CDW gap of $1T$-$TiSe_2$ as a function of temperature.

C. M. thanks Johan Chang for helping aligning the samples. This work was performed at the ADRESS beam line using the SAXES instrument jointly built by Paul Scherrer Institut, Switzerland, and Politecnico di Milano, Italy. This project was partially supported by the Fonds National Suisse pour la Recherche Scientifique through Division II and the Swiss National Center of Competence in Research MaNEP.

*claude.monney@psi.ch

[1] M. Z. Hasan, E. D. Isaacs, Z.-X. Shen, L. L. Miller, K. Tsutsui, T. Tohyama, and S. Maekawa, Science **288**, 1811 (2000).

[2] L. Braicovich, J. van den Brink, V. Bisogni, M. M. Sala, L. J. P. Ament, N. B. Brookes, G. M. De Luca, M. Salluzzo, T. Schmitt, V. N. Strocov, and G. Ghiringhelli, Phys. Rev. Lett. **104**, 077002 (2010).

[3] J. Schlappa, T. Schmitt, F. Vernay, V. N. Strocov, V. Ilakovac, B. Thielemann, H. M. Ronnow, S. Vanishri, A. Piazzalunga, X. Wang, L. Braicovich, G. Ghiringhelli, C. Marin, J. Mesot, B. Delley, and L. Patthey, Phys. Rev. Lett. **103**, 047401 (2009).

[4] J. Schlappa, K. Wohlfeld, K. J. Zhou, M. Mourigal, M. W. Haverkort, V. N. Strocov, L. Hozoi, C. Monney, S. Nishimoto, S. Singh, A. Revcolevschi, J.-S. Caux, L. Patthey, H. M. Ronnow, J. van den Brink, and T. Schmitt, Nature (London) **485**, 82 (2012).

[5] M. Le Tacon, G. Ghiringhelli, J. Chaloupka, M. Moretti Sala, V. Hinkov, M. W. Haverkort, M. Minola, M. Bakr, K. J. Zhou, S. Blanco-Canosa, C. Monney, Y. T. Song, G. L. Sun, C. T. Lin, G. M. De Luca, M. Salluzzo, G. Khaliullin, T. Schmitt, L. Braicovich, and B. Keimer, Nature Phys. **7**, 725 (2011).

[6] L. J. P. Ament, M. van Veenendaal, T. P. Devereaux, and J. van den Brink, Rev. Mod. Phys. **83**, 705 (2011).

[7] V. N. Strocov, T. Schmitt, J.-E. Rubensson, P. Blaha, T. Paskova, and P. O. Nilsson, Phys. Rev. B **72**, 085221 (2005).

[8] Y. Ma, N. Wassdahl, P. Skytt, J. Guo, J. Nordgren, P. D. Johnson, J-E. Rubensson, T. Boske, W. Eberhardt, and S. D. Kevan, Phys. Rev. Lett. **69**, 2598 (1992); J. A. Carlisle, E. L. Shirley, E. A. Hudson, L. J. Terminello, T. A. Callcott, J. J. Jia, D. L. Ederer, R. C. C. Perera, and F. J. Himpsel, *ibid.* **74**, 1234 (1995); S. Shin, A. Agui, M. Watanabe, M. Fujisawa, Y. Tezuka, and T. Ishii, Phys. Rev. B **53**, 15 660 (1996).

[9] V. N. Strocov, T. Schmitt, U. Flechsig, T. Schmidt, A. Imhof, Q. Chen, J. Raabe, R. Betemps, D. Zimoch, J. Krempasky, X. Wang, M. Grioni, A. Piazzalunga, and L. Patthey, J. Synchrotron Radiat. **17**, 631 (2010).

[10] G. Ghiringhelli, A. Piazzalunga, C. Dallera, G. Trezzi, L. Braicovich, T. Schmitt, V. N. Strocov, R. Betemps, L. Patthey, X. Wang, and M. Grioni, Rev. Sci. Instrum. **77**, 113108 (2006).

[11] F. J. Di Salvo, D. E. Moncton, and J. V. Waszczak , Phys. Rev. B **14**, 4321 (1976).

[12] H. Cercellier *et al.*, Phys. Rev. Lett. **99**, 146403 (2007).

[13] J. van Wezel, P. Nahai-Williamson, and S. S. Saxena, Phys. Rev. B **83**, 024502 (2011).

[14] T. E. Kidd, T. Miller, M. Y. Chou, and T. C. Chiang, Phys. Rev. Lett. **88**, 226402 (2002).

[15] K. Rossnagel, L. Kipp, and M. Skibowski, Phys. Rev. B **65**, 235101 (2002).

[16] C. Monney, E. F. Schwier, M. G. Garnier, N. Mariotti, C. Didiot, H. Beck, P. Aebi, H. Cercellier, J. Marcus, C. Battaglia, H. Berger, and A. N. Titov, Phys. Rev. B **81**, 155104 (2010).

[17] C. Monney, G. Monney, P. Aebi, and H. Beck, Phys. Rev. B **85**, 235150 (2012).

[18] C. Monney, H. Cercellier, F. Clerc, C. Battaglia, E. F. Schwier, C. Didiot, M. G. Garnier, H. Beck, P. Aebi, H. Berger, L. Forrò, and L. Patthey, Phys. Rev. B **79**, 045116 (2009).

[19] K. J. Zhou, M. Radovic, J. Schlappa, V. Strocov, R. Frison, J. Mesot, L. Patthey, and T. Schmitt, Phys. Rev. B **83**, 201402(R) (2011).

[20] A typical calculated XAS spectrum of a d^1 system in an octahedral crystal field can be seen in Ref. [21].

[21] F. M. F. de Groot, J. C. Fuggle, B. T. Thole, and G. A. Sawatzky, Phys. Rev. B **42**, 5459 (1990).

[22] M. Calandra and F. Mauri, Phys. Rev. Lett. **106**, 196406 (2011).

[23] C. Monney, C. Battaglia, H. Cercellier, P. Aebi, and H. Beck, Phys. Rev. Lett. **106**, 106404 (2011).

[24] T. Hahn, Comput. Phys. Commun. **168**, 78 (2005).

[25] $\epsilon_v^0 = 0.03\,\text{eV}$, $\epsilon_b^0 = -0.04\,\text{eV}$, $t_v = 0.06$ eV, $t_c = 0.03$ eV, $m_v = -0.23m_e$, $m_{c_x} = 5.5m_e$, and $m_{c_y} = 0.5m_e$ (m_e is the bare electron mass).

[26] Another Gaussian has been added at zero energy loss for reproducing the elastic line.

[27] We have fitted the low energy part of the RIXS spectra at $Q_{\parallel} = 0.01\Gamma M$ with Gaussians, having previously subtracted the elastic line.

[28] G. Li, W. Z. Hu, D. Qian, D. Hsieh, M. Z. Hasan, E. Morosan, R. J. Cava, and N. L. Wang, Phys. Rev. Lett. **99**, 027404 (2007).

[29] S. Eisebitt and W. Eberhardt, J. Electron Spectrosc. Relat. Phenom. **110**, 335 (2000).